Cortical dynein is critical for proper spindle positioning in human cells

Sachin Kotak, Coralie Busso, and Pierre Gönczy

Swiss Institute for Experimental Cancer Research (ISREC), School of Life Sciences, Swiss Federal Institute of Technology Lausanne (EPFL), Lausanne CH-1015, Switzerland

Correct spindle positioning is fundamental for proper cell division during development and in stem cell lineages. Dynein and an evolutionarily conserved ternary complex (nuclear mitotic apparatus protein [NuMA]–LGN–Gα in human cells and LIN-5–GPR-1/2–Gα in *Caenorhabditis elegans*) are required for correct spindle positioning, but their relationship remains incompletely understood. By analyzing fixed specimens and conducting live-imaging experiments, we uncovered that appropriate levels of ternary complex components are critical for dynein-dependent spindle positioning in HeLa cells and *C. elegans* embryos. Moreover, using mutant versions of Gα in both systems, we established that dynein acts at the membrane to direct spindle positioning. Importantly, we identified a region within NuMA that mediates association with dynein. By using this region to target dynein to the plasma membrane, we demonstrated that the mere presence of dynein at that location is sufficient to direct spindle positioning in HeLa cells. Overall, we propose a model in which the ternary complex serves to anchor dynein at the plasma membrane to ensure correct spindle positioning.

Introduction

Correct spindle position is an essential feature of cell division from yeast to man. In animal cells, the cleavage furrow is specified so as to bisect the mitotic spindle. Therefore, correct orientation of the spindle along a given axis, as well as its accurate placement on this axis (hereafter collectively referred to as "spindle positioning" for simplicity), is critical for dictating the relative size of daughter cells and for ensuring the proper distribution of cytoplasmic constituents at cell division. Spindle positioning plays an important role during development of metazoan organisms, as well as in stem cell lineages. Despite important progress in recent years, the mechanisms governing spindle positioning remain incompletely understood.

Molecules important for spindle positioning have been identified notably in invertebrate systems, including *Drosophila melanogaster* neuroblasts and *Caenorhabditis elegans* embryos (reviewed by Gönczy, 2008, Knoblich, 2008; Siller and Doe, 2009). In *C. elegans* one-cell stage embryos, for instance, forward genetic and RNAi-based functional genomic screens have uncovered that a ternary complex, as well as the minus end–directed motor dynein, is essential for generating pulling forces that act on astral microtubules to position the spindle. This ternary complex comprises the partially redundant heterotrimeric Gα proteins GOA-1 and GPA-16 and the essentially identical GoLoco proteins GPR-1 and GPR-2 (hereafter collectively referred as GPR-1/2) as well as the coiled-coil domain protein LIN-5 (Gotta and Ahringer, 2001; Colombo et al., 2003; Gotta et al., 2003; Srinivasan et al., 2003; Nguyen-Ngoc et al., 2007).

Dynein is a multisubunit AAA ATPase motor protein complex of >1.5 MD that is fundamental for several cellular processes across eukaryotic evolution, including proper organelle distribution, spindle assembly, and kinetochore function (reviewed by Kardon and Vale, 2009). This complex comprises the dynein heavy chain motor protein and dynein intermediate and light chains, as well as several additional factors, including the dynactin complex that is needed for dynein activity. In *C. elegans* embryos, coimmunoprecipitation experiments indicate that the ternary complex associates with dynein (Couwenbergs et al., 2007; Nguyen-Ngoc et al., 2007; Park and Rose, 2008). Moreover, the presence of dynein at the cell cortex is compromised upon depletion of ternary complex components in early worm embryos (Nguyen-Ngoc et al., 2007). Together, these observations have led to a working model in which the ternary complex would bring dynein to the plasma membrane owing to

Correspondence to Pierre Gönczy: Pierre.Gonczy@epfl.ch

Abbreviations used in this paper: DIC, dynein intermediate chain; NuMA, nuclear mitotic apparatus protein; siRNA, silencing-induced RNA.

The Rockefeller University Press $30.00
J. Cell Biol. Vol. 199 No. 1 97–110
www.jcb.org/cgi/doi/10.1083/jcb.201203166

myristoylation of the Gα moiety (reviewed by Gönczy, 2008). Such anchored dynein would then generate a pull on astral microtubules by attempting to move toward their minus end and/or maintain an association with force-generating depolymerizing microtubules. However, whether dynein acts at the cell membrane has not been determined. Moreover, whether the ternary complex exerts a function besides anchoring dynein to the cell cortex has also not been addressed.

Work in other systems, including human cells in culture, indicates that the role of the ternary complex in spindle positioning is evolutionarily conserved. Thus, nuclear mitotic apparatus protein [NuMA]–LGN–Gαi, which are related to LIN-5–GPR-1/2–Gα, are needed for spindle positioning in polarized vertebrate cells (Du and Macara, 2004; Lechler and Fuchs, 2005; Zheng et al., 2010; Peyre et al., 2011; Williams et al., 2011). This requirement extends to nonpolarized HeLa cells, in which spindle position can be assayed using a fibronectin substratum (Woodard et al., 2010; Kiyomitsu and Cheeseman, 2012). In this case, cortical landmarks present during interphase in cells grown on a uniform fibronectin coating or on fibronectin-based micropatterns impart spindle position during mitosis in a predictable manner (Théry et al., 2005; Toyoshima and Nishida, 2007). Just like in one-cell stage *C. elegans* embryos, dynein is important for spindle positioning in HeLa cells (Kiyomitsu and Cheeseman, 2012). However, as in *C. elegans*, the relationship between dynein and the ternary complex is also not fully understood in human cells. Here, conducting experiments in human cells in culture and in *C. elegans* embryos, we provide evidence that dynein can function at the plasma membrane independently of the ternary complex and that is compatible with the notion that the sole role of the ternary complex in spindle positioning is to anchor dynein at that location.

Results

Appropriate levels of ternary complex components are critical for proper spindle positioning in HeLa cells

We set out to investigate the relationship between components of the ternary complex (NuMA–LGN–Gαi) and dynein during spindle positioning in HeLa cells. To this end, we monitored spindle position using coverslips uniformly coated with fibronectin. In control conditions, this usually directs the metaphase spindle to align parallel to the substratum (Fig. 1 A and Fig. S1, A and B; Toyoshima and Nishida, 2007). In contrast, we found that silencing-induced RNA (siRNA)–mediated depletion of three Gαi proteins ($G\alpha i_{1-3}$), of LGN, of NuMA, or of the dynein heavy chain DYNC1H1 results in the spindle adopting a significantly more random position (Fig. S1, C–F). The same is true of cells treated with pertussis toxin, which ADP ribosylates and thus inactivates $G\alpha_i$ proteins (Fig. S1 G; Woodard et al., 2010). These results are consistent with and extend findings showing that $G\alpha i_{1-3}$, LGN, and dynein are needed for proper spindle positioning in HeLa cells (Woodard et al., 2010; Kiyomitsu and Cheeseman, 2012).

In polarized MDCK cells, overexpression of Gαi or LGN results in the metaphase spindle exhibiting excess oscillations

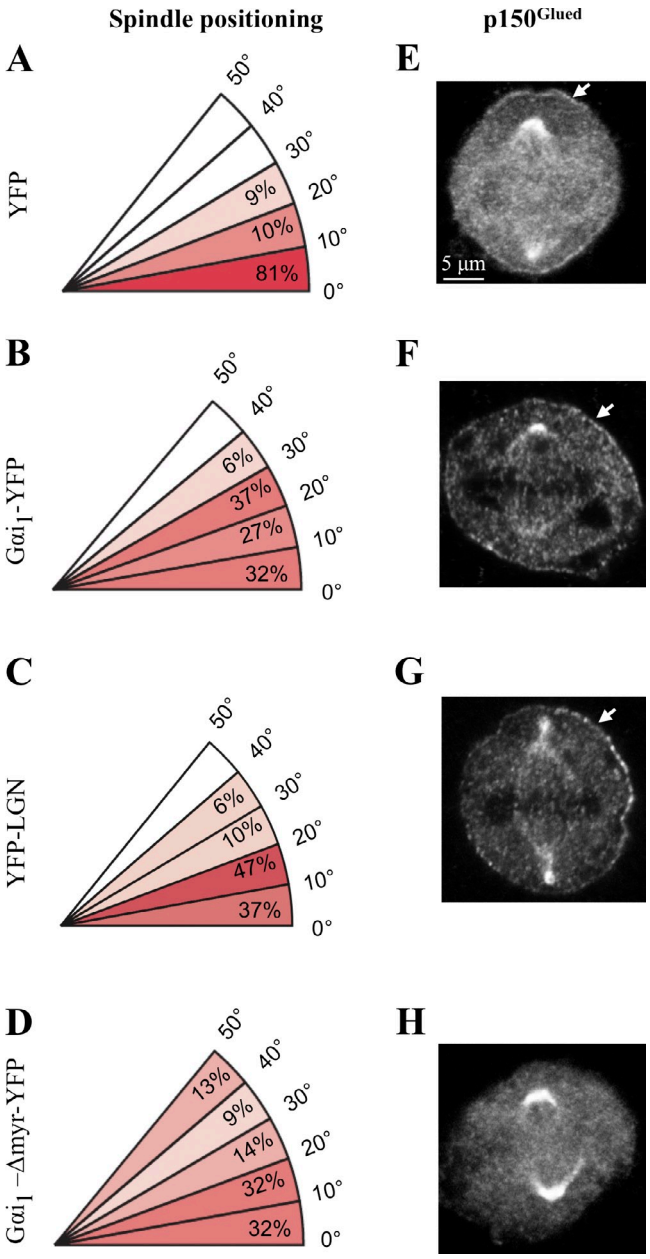

Figure 1. **Appropriate levels of ternary complex components are necessary for proper spindle positioning in HeLa cells.** (A–D) Distribution of metaphase spindle angles with respect to the fibronectin substratum in cells transfected with YFP (A), $G\alpha i_1$-YFP (B), YFP-LGN (C), or $G\alpha i_1$-Δmyr-YFP (D). A minimum of 40 cells was analyzed for each condition, and the significance was compared with control cells (YFP) using a two-tailed Student's *t* test; in all three experimental conditions, $P < 0.001$. (E–H) HeLa cells transfected for 36 h with YFP (E), $G\alpha i_1$-YFP (F), YFP-LGN (G), or $G\alpha i_1$-Δmyr-YFP (H) and stained for the dynactin subunit $p150^{Glued}$. Arrows point to cortical $p150^{Glued}$. Over 95% of cells transfected with $G\alpha i_1$-YFP (F) or YFP-LGN (G) exhibited more extensive $p150^{Glued}$ signal at the cell cortex than those transfected with YFP alone (E; $n > 100$ in each condition, except for H, in which $n = 32$).

(Du and Macara, 2004), but whether this is accompanied by alterations in cortical dynein has not been investigated. We addressed this question in nonpolarized HeLa cells. As shown in Fig. 1 (B and C), we found that overexpression of $G\alpha i_1$-YFP or YFP-LGN leads to defective spindle positioning on uniform fibronectin-coated coverslips. Accordingly, live imaging of HeLa

cells expressing GFP–α-tubulin and mCherry-H2B reveals that whereas the metaphase spindle does not exhibit much movements in control conditions (Fig. 2 A and Video 1, S1), dramatic oscillations are caused by excess $G\alpha i_1$-YFP or YFP-LGN (Fig. 2, B and C; and Video 1, S2 and S3; see also Video 2 with faster acquisition regime). Importantly, we found that whereas in control conditions the dynactin component $p150^{Glued}$ is present at the cell cortex in a restricted manner above the spindle poles (Fig. 1 E), overexpression of $G\alpha i_1$-YFP or YFP-LGN leads to an increase and expansion of cortical $p150^{Glued}$ (Fig. 1, F and G). Analogous results were obtained by examining the distribution of the dynein intermediate chain (DIC; unpublished data). We conclude that overexpression of $G\alpha i_1$-YFP or YFP-LGN results in spindle positioning defects that correlate with the presence of excess cortical dynein.

We next addressed whether excess dynein is causative of the spindle positioning defects observed upon $G\alpha i_1$-YFP or YFP-LGN overexpression. To this end, we partially depleted $p150^{Glued}$ in cells overexpressing $G\alpha i_1$-YFP or YFP-LGN. Importantly, we found that such depletion abrogates the exaggerated spindle oscillations observed upon $G\alpha i_1$-YFP or YFP-LGN overexpression (Fig. 2, D and E, compare with B and C; and Video 3, S7 and S8). Similar results were obtained upon partial depletion of the dynein heavy chain DYNC1H1 in cells overexpressing $G\alpha i_1$-YFP or YFP-LGN (Fig. S2, A and B; compare with Fig. 2, B and C; and Video 3, S9 and S10). Together, these findings demonstrate that appropriate levels of ternary complex components are critical for proper spindle positioning and that the impact of excess ternary complex on this process is mediated through dynein.

The ternary complex is needed at the membrane to direct spindle positioning in HeLa cells and in *C. elegans* embryos

We set out to investigate whether dynein is required at the plasma membrane or instead elsewhere in the cell to direct spindle positioning. Although ternary complex components are needed for the presence of dynein at the plasma membrane in *C. elegans* and human cells (this study; Nguyen-Ngoc et al., 2007; Woodard et al., 2010; Kiyomitsu and Cheeseman, 2012), dynein located in the cytoplasm and associated with endomembranes has also been proposed to mediate microtubule length–dependent forces in some settings (see for example Wühr et al., 2009; Kimura and Kimura, 2011).

To address whether dynein is required at the plasma membrane to direct spindle positioning in HeLa cells, we overexpressed a mutant form of $G\alpha i_1$ lacking two N-terminal amino acids that ensure myristoylation and palmitoylation of the protein ($G\alpha i_1$-Δmyr-YFP). We anticipated that overexpression of such a mutant form that cannot localize to the plasma membrane should compete with endogenous Gαi for interaction with other ternary complex components, as well as dynein, and may thus affect spindle positioning. As expected, in contrast to $G\alpha i_1$-YFP, which is enriched at the plasma membrane (Fig. 2 B), we found that $G\alpha i_1$-Δmyr-YFP is present throughout the cytoplasm (Fig. 2 F). As anticipated also, we found that $p150^{Glued}$ is no longer present at the cell cortex in such cells (Fig. 1 H). Analysis of fixed specimens on uniform fibronectin-coated coverslips indicates that spindle positioning is defective upon overexpression of $G\alpha i_1$-Δmyr-YFP (Fig. 1 D), whereas live-imaging experiments reveal that the spindle hardly moves during metaphase (Fig. 2 F and Video 4). We conclude that membrane localization of dynein is necessary for proper spindle positioning in HeLa cells.

We investigated whether the aforementioned mechanisms are evolutionarily conserved. In *C. elegans* embryos, overexpression of the LGN-relative GPR-1 fused to YFP results in excess spindle oscillations in the one-cell stage (Fig. 3 D, compare with C; and Video 5, S12 and S13; Redemann et al., 2011). Importantly, we found a substantial increase in the amount of the dynein heavy chain DHC-1 at the cell cortex in one-cell stage embryos overexpressing YFP–GPR-1 (Fig. 3 B, compare with A). Interestingly, in addition, this revealed an asymmetry in the distribution of cortical dynein, with more protein present on the posterior side, in line with the fact that a larger net pulling force is exerted on that side (reviewed by Gönczy, 2008). To test whether excess spindle oscillations in such embryos are caused by dynein activity, we partially depleted DHC-1 by RNAi in embryos overexpressing YFP–GPR-1. As reported in Fig. 3 E and Video 5 (S14), we found that this drastically reduces spindle oscillations. These findings establish that, just like in human cells, the impact of the ternary complex on spindle positioning is mediated through dynein in *C. elegans*.

To address whether dynein is likewise required at the plasma membrane in *C. elegans*, we made use of *goa-1*(*n1134*) mutant animals, which lack the four N-terminal–most amino acids of GOA-1 and are thus devoid of the myristoylation and palmitoylation consensus (Mendel et al., 1995). As expected, in contrast to the wild-type, GOA-1 protein does not localize to the plasma membrane in one-cell stage *goa-1*(*n1134*) embryos (Fig. 4 B, compare with A), despite overall protein levels being unchanged (not depicted). As anticipated also, we found that DHC-1 levels at the cell cortex are substantially decreased in *goa-1*(*n1134*) embryos simultaneously depleted of the partially redundant Gα protein GPA-16 (Fig. 4 D, compare with C). Importantly, in addition, analysis by time-lapse differential interference contrast microscopy revealed that the spindle is positioned symmetrically in *goa-1*(*n1134*) *gpa-16*(*RNAi*) embryos, as is the case in embryos carrying the null allele *goa-1*(*sa734*) and subjected to *gpa-16* RNAi (Fig. 4, E–G; and Video 6). We conclude that membrane localization of dynein is necessary for proper spindle positioning also in *C. elegans*.

NuMA interacts with dynein through its N-terminal part

We wanted to address whether, in addition to being necessary, dynein is also sufficient to mediate spindle positioning in HeLa cells. To this end, we sought to generate conditions in which dynein could be targeted experimentally to the plasma membrane. This would then enable us to address whether dynein can function in the absence of the ternary complex to direct spindle positioning. Because dynein is a large multisubunit complex difficult to dissect through a systematic structure/function analysis, we set out instead to identify a region within a potential

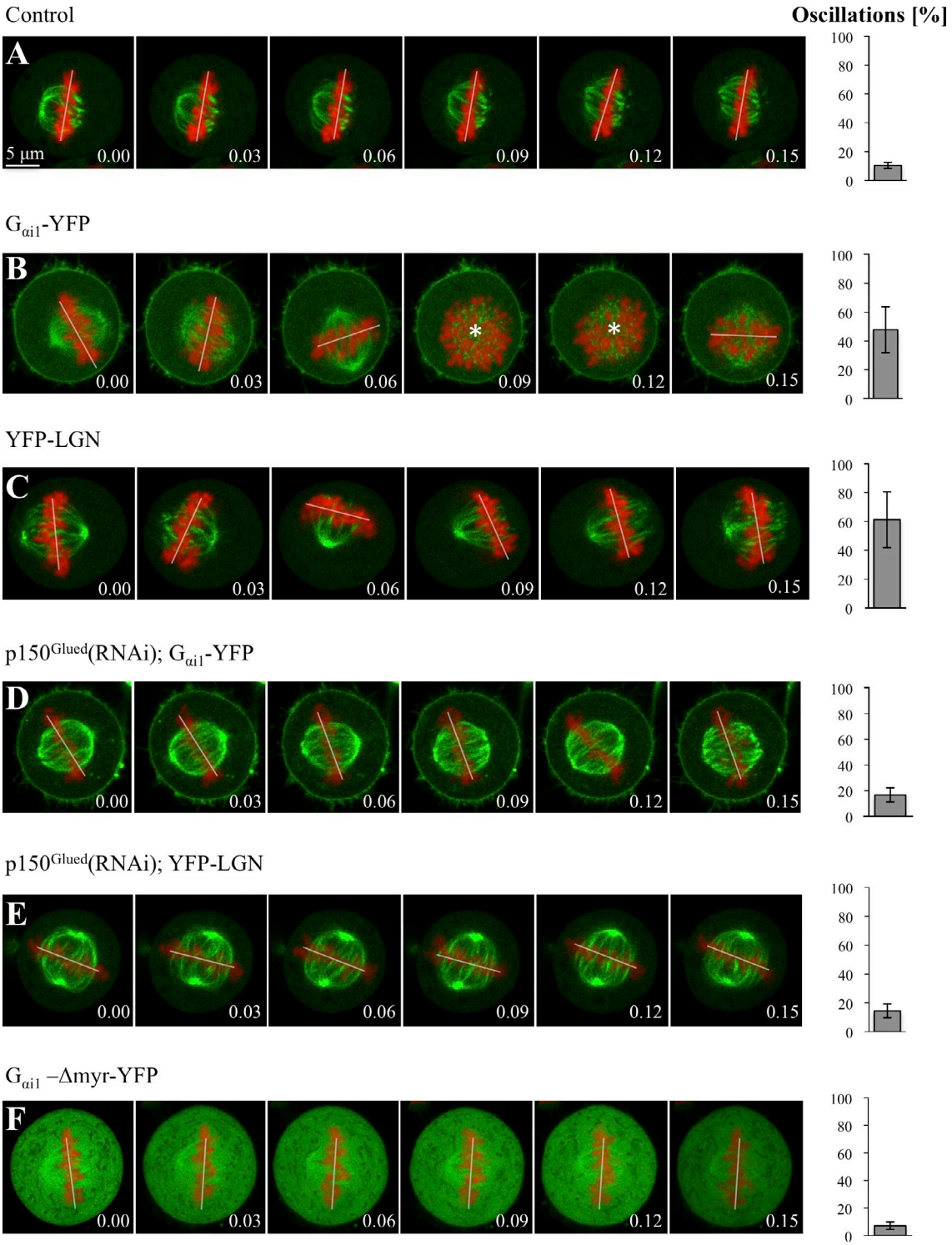

Figure 2. **Dynein is necessary for ternary complex–induced spindle oscillations in HeLa cells.** (A–F) Images from time-lapse microscopy of metaphase HeLa Kyoto cells stably expressing GFP–α-tubulin as well as mCherry-H2B and transfected with YFP (A), $G\alpha i_1$-YFP (B), YFP-LGN (C), $G\alpha i_1$-YFP and p150^{Glued} siRNAs (D), YFP-LGN and p150^{Glued} siRNAs (E), or $G\alpha i_1$-Δmyr-YFP (F; see also Videos 1–4). Note that cortical YFP-LGN, which is present at low levels, is not visible in C and E because of the strong GFP–α-tubulin signal but can be seen better in Video 1 (S4), in which YFP-LGN is transfected in HeLa Kyoto cells expressing solely mCherry-H2B. In this and other figures with time-lapse sequences, the position of chromosomes is indicated by a white line when chromosomes are within the imaging plane and by an asterisk when the metaphase plate is no longer in the plane of view. 10 cells were imaged for each condition. The bar graphs on the right are readouts of the extent of spindle oscillations, representing the frequency at which chromosome position changes >10° between two frames (including when they move out of the imaging plane), along with the SEM. Two-tailed Student's *t* tests show that the extent of spindle oscillations upon overexpression of $G\alpha i_1$-YFP or of YFP-LGN is statistically different from that observed in control conditions; in both cases, $P < 0.0001$. Similarly, the values in $G\alpha i_1$-YFP and p150^{Glued} siRNA (D), as well as in YFP-LGN and p150^{Glued} siRNA (E), are statistically different from those of $G\alpha i_1$-YFP (B) or YFP-LGN (C) overexpression alone; in both cases, $P < 0.0005$. In contrast, the values in $G\alpha i_1$-YFP and p150^{Glued} siRNA (D), as well as in YFP-LGN and p150^{Glued} siRNA (E), are not statistically different from those in the control condition (A); $P = 0.16$ and $P = 0.18$, respectively. Time is indicated in hours and minutes.

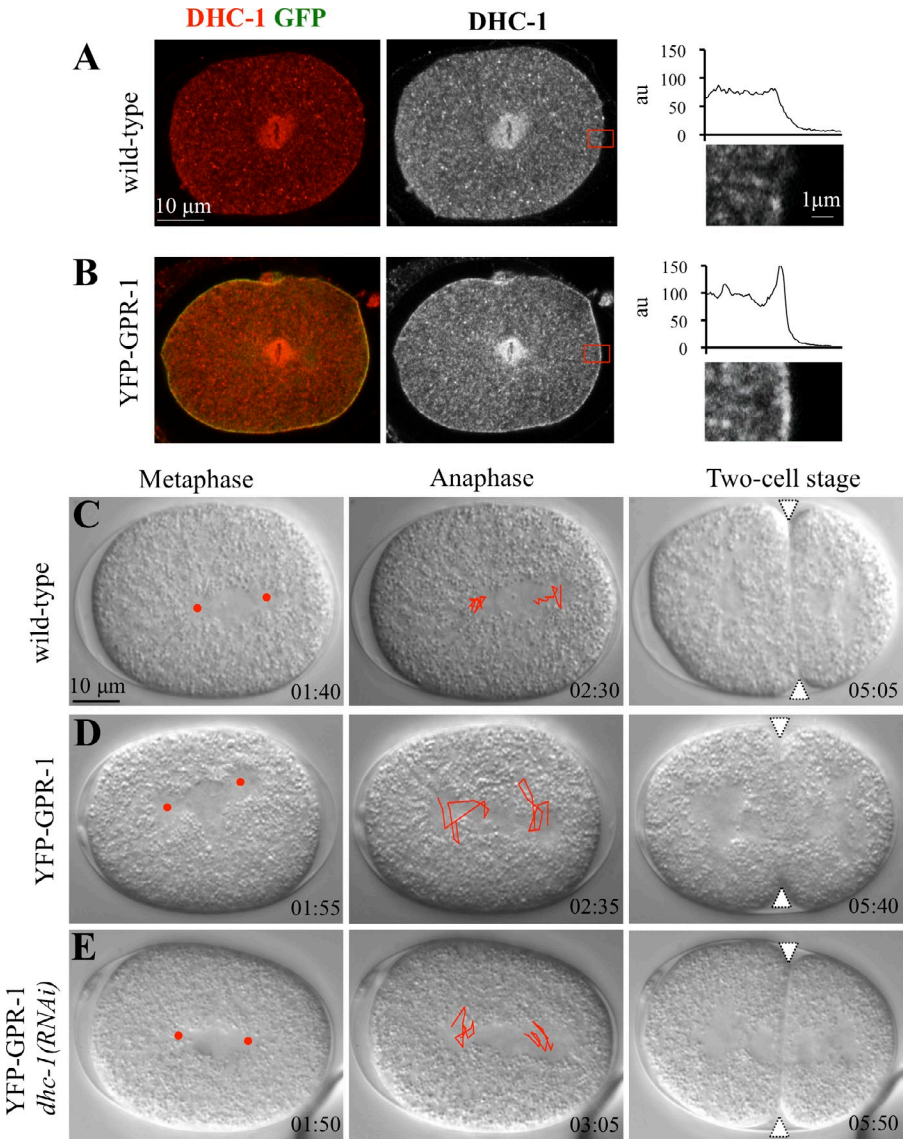

Figure 3. **Dynein functions downstream of GPR-1/2 in directing spindle positioning in *C. elegans*.** (A and B) Wild-type (A) or YFP–GPR-1 (B) one-cell stage embryo stained for DHC-1 (shown in red in merge and alone on the right) and GFP (green in merge). On the very right, higher magnifications of the cortical regions (represented by red boxes) shown in A and B highlight the presence of excess DHC-1 at the cell membrane upon YFP–GPR-1 expression (B, compare with A). The corresponding line scan of pixel intensities (in arbitrary units [au]) across these cortical regions is shown for one representative embryo. 10 embryos were scored for each condition. (C–E) Images from time-lapse DIC microscopy of *C. elegans* embryos from metaphase in the one-cell stage (left), through anaphase in the one-cell stage (middle), and in the early two-cell stage (right), either wild type (C), expressing YFP–GPR-1 (D), or expressing YFP–GPR-1 and subjected to partial *dhc-1*(*RNAi*) in addition (E). See also corresponding Video 5. Elapsed time is indicated in minutes and seconds, with t = 0 corresponding to nuclear envelope breakdown. Red discs and white triangles indicate the position of centrosomes during metaphase and the cleavage furrow, respectively. Spindle pole movements were tracked during 1 min, starting 2 min before the onset of cytokinesis, and are represented on the anaphase embryos. Note excess spindle movements in embryo expressing YFP–GPR-1, which are significantly dampened by partial *dhc-1*(*RNAi*). 10 embryos of each condition were analyzed.

dynein-interacting component that could recruit the entire complex to the plasma membrane. Given that NuMA associates with dynein in *Xenopus laevis* egg extract (Merdes et al., 1996), this protein was an attractive candidate for this purpose.

We carried coimmunoprecipitation experiments using extracts from a stable cell line expressing the DIC fused to GFP (Kobayashi and Murayama, 2009). This revealed that the dynein complex associates with NuMA in human cells (Fig. S3 A), in line with recent findings showing that LGN interacts with NuMA and dynein in HeLa cell extracts (Kiyomitsu and Cheeseman, 2012).

NuMA is a 2,115–amino acid–long protein that contains a poorly characterized N-terminal part followed by an extended coiled-coil domain and a C-terminal moiety (Fig. 5 A). This latter part contains evolutionarily conserved interaction domains with LGN and with microtubules, as well as the NLS responsible for the presence of NuMA in the nucleus during interphase. To investigate which part of NuMA associates with the dynein complex, we divided the protein into three fragments (Fig. 5 A), fused them to GFP, and examined their distribution upon transient transfection. As shown in Fig. S3 (B–D), we found that during interphase both GFP-NuMA(1–705) and GFP-NuMA(706–1,410) are present in the cytoplasm, whereas GFP-NuMA(1,411–2,115) localizes mainly to the nucleus, as expected from the presence of the NLS within this fragment (Gueth-Hallonet et al., 1996). During mitosis, GFP-NuMA (1–705) and GFP-NuMA(706–1,410) are present in the cytoplasm, whereas GFP-NuMA(1,411–2,115) localizes to spindle poles and to the cell cortex, as anticipated from its ability to interact with microtubules and LGN (Fig. S3, E–G).

We set out to identify which fragment of NuMA associates with dynein using three complementary approaches. First, we predicted that overexpression of a NuMA fragment that interacts with the dynein complex might sequester it away from spindle poles and the plasma membrane during mitosis. Suggestively, we found this to be the case upon overexpression of GFP-NuMA(1–705), whereas overexpression of the other two fragments does not displace dynein from spindle poles (Fig. 5, B–E). We noted also that GFP-NuMA(1,411–2,115) overexpression led to a loss of dynein at the plasma membrane (Fig. 5 E),

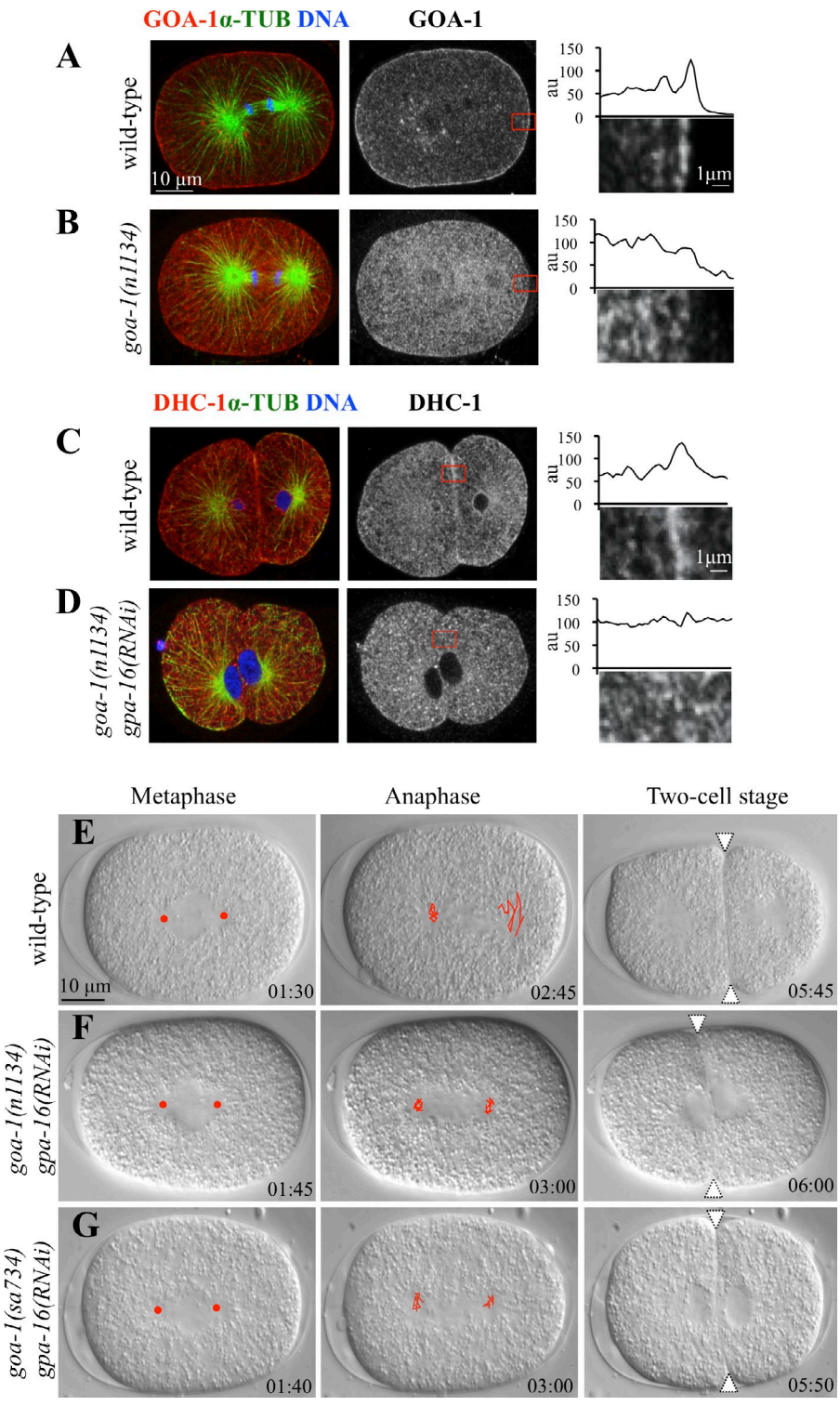

Figure 4. **Gα is required at the membrane to direct spindle positioning in *C. elegans* embryos.** (A and B) Wild-type (A) or *goa-1(n1134)* (B) one-cell stage embryos stained with antibodies against GOA-1 and α-tubulin. Higher magnifications of cortical regions (red boxes) and accompanying line scans of representative embryos are given as in Fig. 3 and highlight the presence (A) or absence (B) of GOA-1. 10 cells were scored for each condition. (C and D) Wild-type (C) or *goa-1(n1134) gpa-16(RNAi)* (D) two-cell stage embryos stained with antibodies against DHC-1 and α-tubulin. Higher magnifications of cortical regions (red boxes) and accompanying line scans of representative embryos are given as in Fig. 3 and highlight the presence (C) or absence (D) of DHC-1. 10 cells were scored for each condition. (E–G) Images from time-lapse DIC microscopy of *C. elegans* embryos from metaphase in the one-cell stage (left) through anaphase in the one-cell stage (middle) and in the early two-cell stage (right) from the wild-type (E), *goa-1(n1134) gpa-16(RNAi)* (F), and *goa-1(sa734) gpa-16(RNAi)* (G; see also corresponding Video 6). Symbols and tracking as described in the legend of Fig. 3. Red discs and white triangles indicate the position of centrosomes during metaphase and the cleavage furrow, respectively. Note equal size of blastomeres in *goa-1(n1134) gpa-16(RNAi)* (F) and *goa-1(sa734) gpa-16(RNAi)* (G) embryos. Time is given in minutes and seconds. au, arbitrary unit; α-TUB, α-tubulin.

probably because this fragment competes with endogenous cortical NuMA for interaction with LGN, without being able to recruit dynein. Second, we anticipated that overexpression of a NuMA fragment that interacts with dynein might result in the dispersal of the Golgi apparatus during interphase, as when dynein function is compromised upon overexpression of the dynactin component p50/dynamitin (Burkhardt et al., 1997). GFP-NuMA(1,411–2,155) was not tested in this assay because it localizes to the nucleus during interphase (Fig. S3 D). Strikingly, we found that whereas the Golgi localizes to the centroid of control interphase cells plated on an L-shape fibronectin-based micropattern (Fig. 5 F), it is completely dispersed upon GFP-NuMA(1–705) overexpression (Fig. 5 G), whereas GFP-NuMA(706–1,410) overexpression is of no consequence (Fig. 5 H). Similar results were obtained with HeLa cells grown on standard coverslips and in nontransformed RPE-1

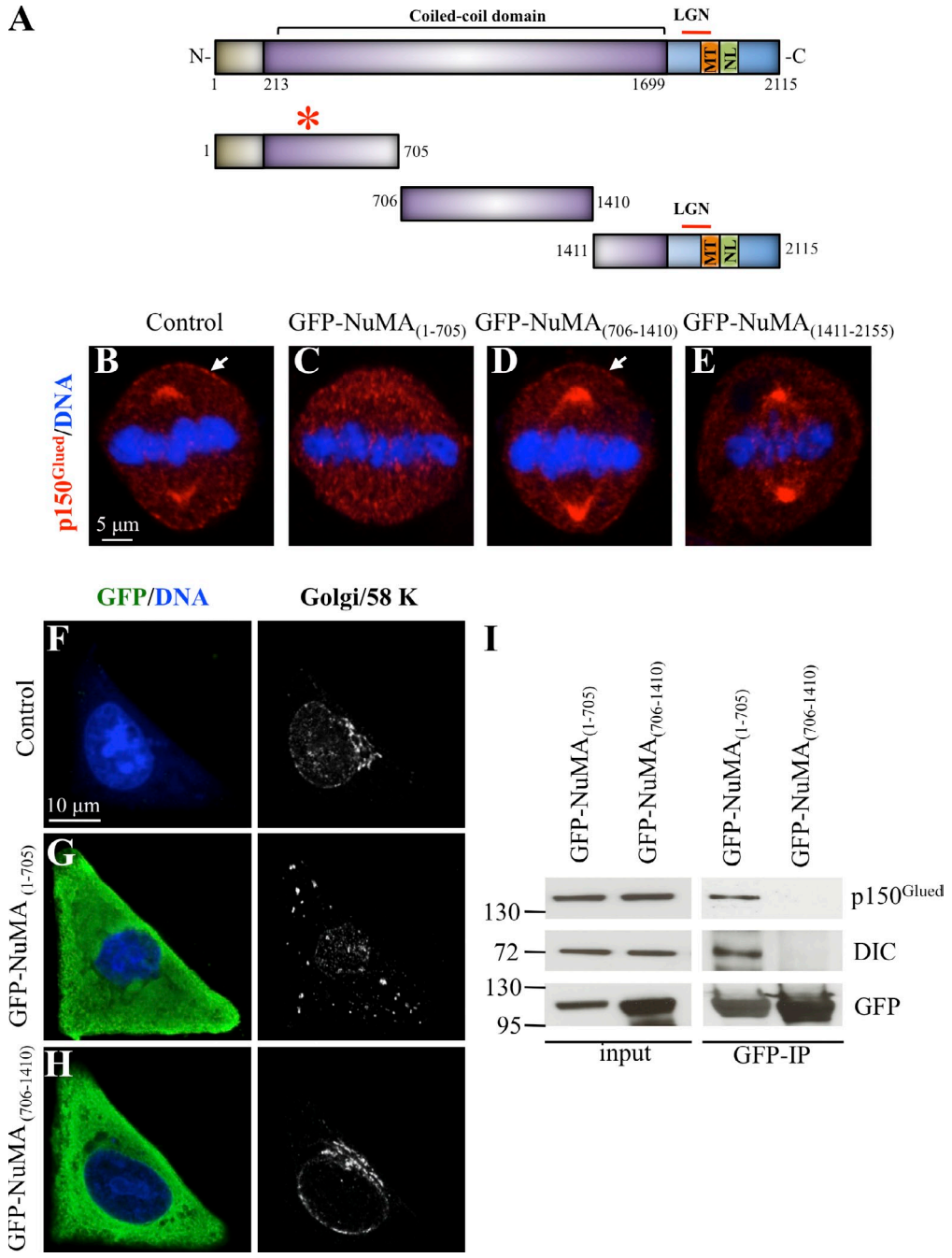

Figure 5. **Mapping of the dynein-interacting domain of NuMA.** (A) Schematic representation of NuMA, with its coil-coiled domain and the regions within its C terminus known to mediate interaction with LGN and microtubules. The NLS is also indicated. The truncated forms for NuMA used in the experiments are depicted on the bottom with their amino acid boundaries. The red asterisk on top of fragment 1–705 denotes interaction with dynein. N, N terminus; C, C terminus. (B–E) Untransfected control HeLa cell (B) or HeLa cells transfected with GFP-NuMA(1–705) (C), GFP-NuMA(706–1,410) (D), or GFP-NuMA(1,411–2,115) (E) and stained for the dynactin subunit p150^{Glued}. Note loss of p150^{Glued} from spindle poles in cells transfected with GFP-NuMA(1–705) and also from the cell membrane in cells transfected either with GFP-NuMA(1–705) (C) or GFP-NuMA(1,411–2,115) (E). 50 cells were scored for each condition. Arrows point to cortical p150^{Glued}. (F–H) Untransfected control HeLa cells (F) or HeLa cells transfected with GFP-NuMA(1–705) (G) or GFP-NuMA(706–1,410) (H) and then transferred to a coverslip with an L-shaped fibronectin micropattern, fixed, and stained with antibodies against GFP and the 58K Golgi marker. Note that the Golgi is dispersed upon transfection of GFP-NuMA(1–705). 30 cells were scored for each condition. (I) Extracts from mitotic cells expressing either GFP-NuMA(1–705) or GFP-NuMA(706–1,410) were immunoprecipitated with GFP-Trap, and the resulting blots were probed for p150^{Glued}, dynein intermediate chain (DIC), and GFP as indicated. Molecular mass is indicated in kilodaltons. IN, input (2% of total); IP, immunoprecipitate (20% of total).

cells (Fig. S3 H and not depicted). Third, coimmunoprecipitation experiments using extracts from mitotic cells confirmed that GFP-NuMA(1–705), but not NuMA(706–1,410), associates with the dynein complex (Fig. 5 I).

Because the N-terminal part of NuMA interacts with Rae1 (Wong et al., 2006), we addressed whether the impact of GFP-NuMA(1–705) on dynein localization is mediated through Rae1. However, Rae1-depleted cells that simultaneously overexpress

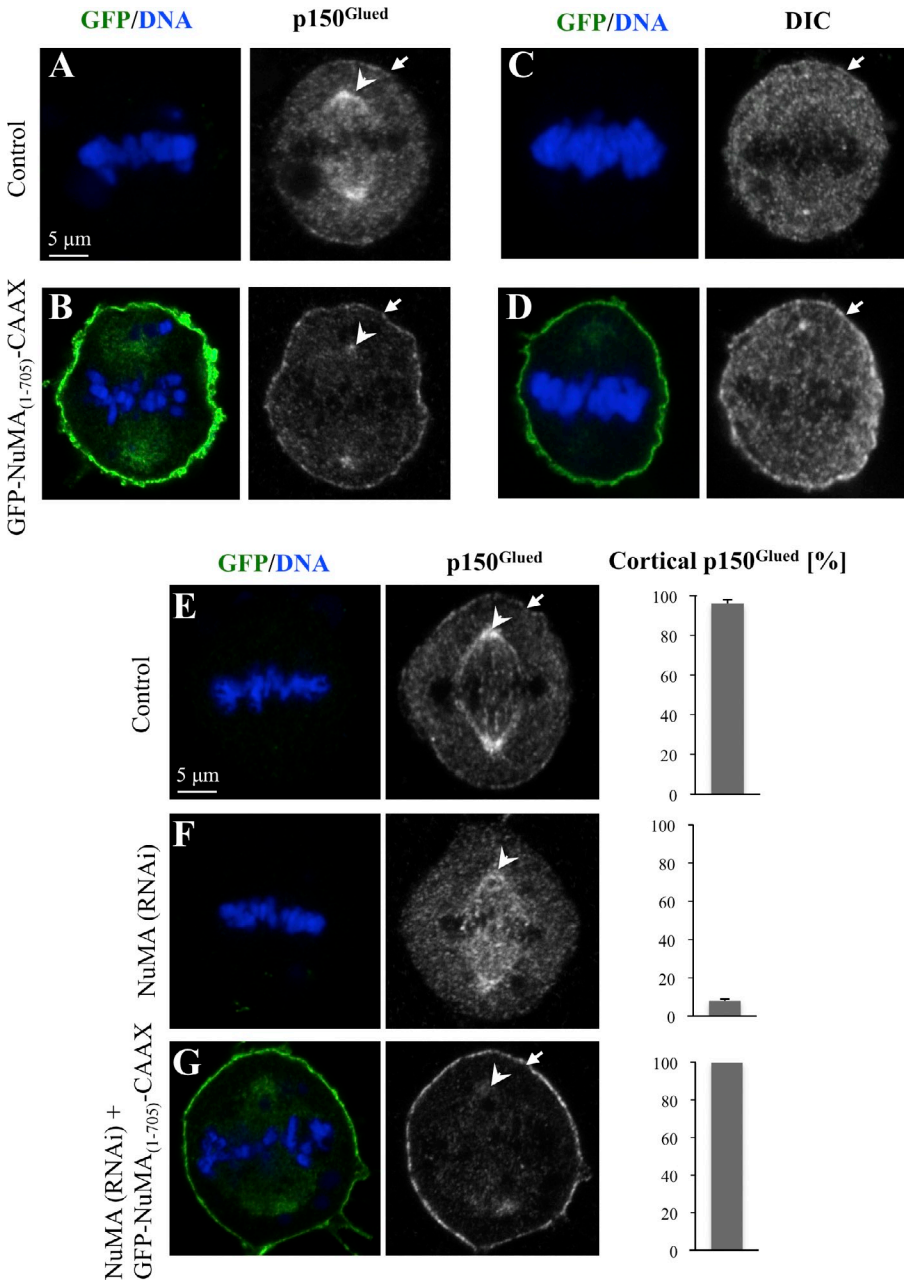

Figure 6. **Targeting GFP-NuMA(1–705) to the plasma membrane recruits dynein to that location.** (A–D) Untransfected control cells (A and C) or cells transfected with GFP-NuMA (1–705)-CAAX (B and D) and stained for the dynactin subunit p150^{Glued} (A and B) or the DIC (C and D) as well as GFP. Arrows point to cortical p150^{Glued} or DIC signals, and arrowheads point to spindle pole p150^{Glued}. 50 cells were scored for each condition. Note the presence of GFP in the vicinity of spindle poles (B), perhaps owing to the presence of endomembranes near spindle poles. (E–G) HeLa cells transfected with control (scrambled siRNAs; E), siRNAs against NuMA (F), or HeLa cell treated with siRNAs against NuMA and also transfected with GFP-NuMA(1–705)-CAAX (G) and stained for GFP (left) and p150^{Glued} (right). The bar graphs on the right represent the percentage of cells with clear cortical p150^{Glued} signal from two independent experiments along with SEM. Arrows point to cortical p150^{Glued}, and arrowheads point to p150^{Glued} at spindle poles. More than 50 cells were scored for each condition in two independent experiments.

GFP-NuMA(1–705) sequester dynein away from spindle poles just like upon overexpression of GFP-NuMA(1–705) alone (Fig. S4 B, compare with A), indicating that the impact of NuMA(1–705) on dynein distribution is Rae1 independent. Overall, these results lead us to conclude that NuMA(1–705) associates with dynein in human cells.

Dynein anchored at the plasma membrane is sufficient for spindle positioning in HeLa cells

Having identified a region of NuMA that associates with dynein and which is distinct from that mediating interaction with LGN and microtubules, we designed an experiment to test whether dynein can function in the absence of the ternary complex to direct spindle positioning. To target dynein to the plasma membrane, we added the CAAX motif from K-ras to GFP-NuMA(1–705), thus generating GFP-NuMA(1–705)-CAAX. As anticipated, cells overexpressing GFP-NuMA(1–705)-CAAX display clear enrichment of GFP at the plasma membrane (Fig. 6 B). Importantly, such cells exhibit high levels of p150^{Glued} at the plasma membrane during mitosis, with a concomitant loss of the signal at spindle poles and in the cytoplasm (Fig. 6 B, compare with A). Similar changes at the plasma membrane were observed when examining the distribution of the DIC (Fig. 6 D, compare with C), indicative of an impact on the whole dynein complex. Because NuMA can form dimers in vitro (Harborth et al., 1995, 1999), in principle, the cortical enrichment of dynein observed upon GFP-NuMA(1–705)-CAAX overexpression might be caused by interaction of the fusion protein with endogenous NuMA. This possibility appears unlikely, however, because GFP-NuMA(1–705) is not present in the nucleus during interphase or at spindle pole during mitosis as would have been expected if

the fusion protein interacted with endogenous NuMA. Nonetheless, to directly test this possibility, we examined p150^{Glued} distribution in cells expressing GFP-NuMA(1–705)-CAAX and simultaneously depleted of endogenous NuMA using siRNA directed against the C terminus, which is absent in the fusion construct. As shown in Fig. 6 G, such cells exhibited a distribution analogous to that of cells overexpressing GFP-NuMA (1–705)-CAAX (compare with Fig. 6 B and see also E and F). Together, these results establish that GFP-NuMA(1–705)-CAAX directly targets dynein to the cell cortex.

Observation of cells overexpressing GFP-NuMA(1–705)-CAAX revealed defects characteristic of compromised dynein function. Thus, we found a fivefold increase in the frequency of binucleated/polyploid cells upon GFP-NuMA(1–705)-CAAX overexpression (Fig. S5 A; Neumann et al., 2010). Furthermore, cells expressing high levels of GFP-NuMA(1–705)-CAAX exhibited a striking phenotype during mitosis with dispersed chromosomes (Fig. S5 B). Similar phenotypes were observed in cells expressing high levels of GFP-NuMA(1–705) (unpublished data), indicating that they are not merely caused by targeting the fusion protein to the cortex, but instead reflect the ability of NuMA(1–705) to interfere with dynein function. We investigated whether the dispersed chromosome phenotype might be linked to loss of dynein components from kinetochores. Accordingly, we found that p150^{Glued} is absent from kinetochores in nocodazole-arrested cells overexpressing high levels of GFP-NuMA(1–705)-CAAX (Fig. S5 D, compare with C). Overall, we conclude that GFP-NuMA(1–705)-CAAX targets dynein to the cell membrane and that high levels of this fusion protein prevent dynein from functioning at other cellular locations.

Next, we analyzed spindle positioning in cells overexpressing GFP-NuMA(1–705)-CAAX to a moderate extent. As shown in Fig. 7 A and Video 7 (S18), we observed exaggerated spindle oscillations during metaphase, as upon overexpression of Gαi_1-YFP or YFP-LGN (compare with Fig. 2, B and C). Spindle morphology and spindle pole organization in these cells appears relatively normal as judged by α-tubulin and Aurora A staining, including the presence of astral microtubules that likely mediate the spindle oscillations (Fig. S5, E and F). To test whether the chromosome congression defects observed upon GFP-NuMA(1–705)-CAAX expression (Fig. 7 A, arrows), presumably because of impaired dynein activity, might be responsible for the exaggerated spindle oscillations, we analyzed spindle positioning in cells overexpressing GFP-NuMA(1–705), which also exhibit defects in chromosome congression (Fig. 7 B, arrows). Importantly, we found that such cells do not exhibit exaggerated spindle oscillations (Fig. 7 B and Video 7, S19), indicating that such exaggerated oscillations upon GFP-NuMA (1–705)-CAAX expression is not a result of defective chromosome congression. We also performed p150^{Glued} depletion in cells overexpressing GFP-NuMA(1–705)-CAAX and found that this significantly dampens the exaggerated spindle oscillations observed upon overexpression of GFP-NuMA(1–705)-CAAX (Fig. 7 C, compare with A; and Video 7, S20). Therefore, the spindle oscillations provoked by GFP-NuMA(1–705)-CAAX overexpression are dynein dependent.

Spindle oscillations upon GFP-NuMA(1–705)-CAAX overexpression occurred without concomitant change in the distribution of ternary complex components, such as LGN (Fig. S5, G and H). We reasoned that if dynein is sufficient for directing spindle positioning, compromising the function of the ternary complex should not abolish exaggerated spindle oscillations upon GFP-NuMA(1–705)-CAAX overexpression. To block the function of the ternary complex in cells overexpressing GFP-NuMA(1–705)-CAAX, we treated cells with pertussis toxin. As shown in Fig. 7 D and Video 8 (S21), the spindle does not exhibit much oscillations in pertussis-treated cells, whereas such oscillations are still observed in cells overexpressing GFP-NuMA(1–705)-CAAX and treated with pertussis toxin, indicating that the spindle oscillations upon overexpression of GFP-NuMA(1–705)-CAAX are independent of ternary complex function (Fig. 7 E and Video 8, S22). Collectively, these findings lead us to conclude that dynein anchored at the plasma membrane is necessary and sufficient for spindle positioning and that the ternary complex serves to place the motor protein complex at that location to dictate proper spindle positioning.

Discussion

In this study, we have established that dynein at the plasma membrane is crucial for proper spindle positioning and that the function of the ternary complex in this process is to ensure appropriate levels of the motor protein complex at this location.

Identification of a region within NuMA that mediates interaction with dynein

It is well established that NuMA and its homologues Mud in *Drosophila* and LIN-5 in *C. elegans* can associate with the dynein complex (Merdes et al., 1996; Nguyen-Ngoc et al., 2007; Siller and Doe, 2009; Radulescu and Cleveland, 2010; Kiyomitsu and Cheeseman 2012). Somewhat surprisingly, however, what region within these proteins mediates this interaction was not known before our work. We found that expression of GFP-NuMA(1–705) interferes with dynein function, presumably because it acts in a dominant-negative fashion by titrating the motor protein away from its normal sites of action. It will be interesting to address whether the related region plays an analogous role in Mud and LIN-5.

There are other sequence motifs besides the one identified here that can mediate interaction with the dynein complex. For instance, the DYNLL1 (dynein light chain 1) recognizes proteins that bear consensus TQT motifs (Rapali et al., 2011). The region that we identified within NuMA to interact with dynein does not contain a TQT motif and is distinct from those that mediate interaction with LGN or microtubules. By adding a CAAX motif to this newly identified region, we targeted GFP-NuMA(1–705) to the plasma membrane and thus displaced substantial amounts of dynein from the spindle poles and the cytoplasm to the plasma membrane. As a result, we observed dramatic phenotypes, including Golgi dispersal, loss of kinetochore function, and cell division failure, all of which mimic phenotypes observed when dynein function is inactivated using siRNAs or after overexpression of the dynactin component

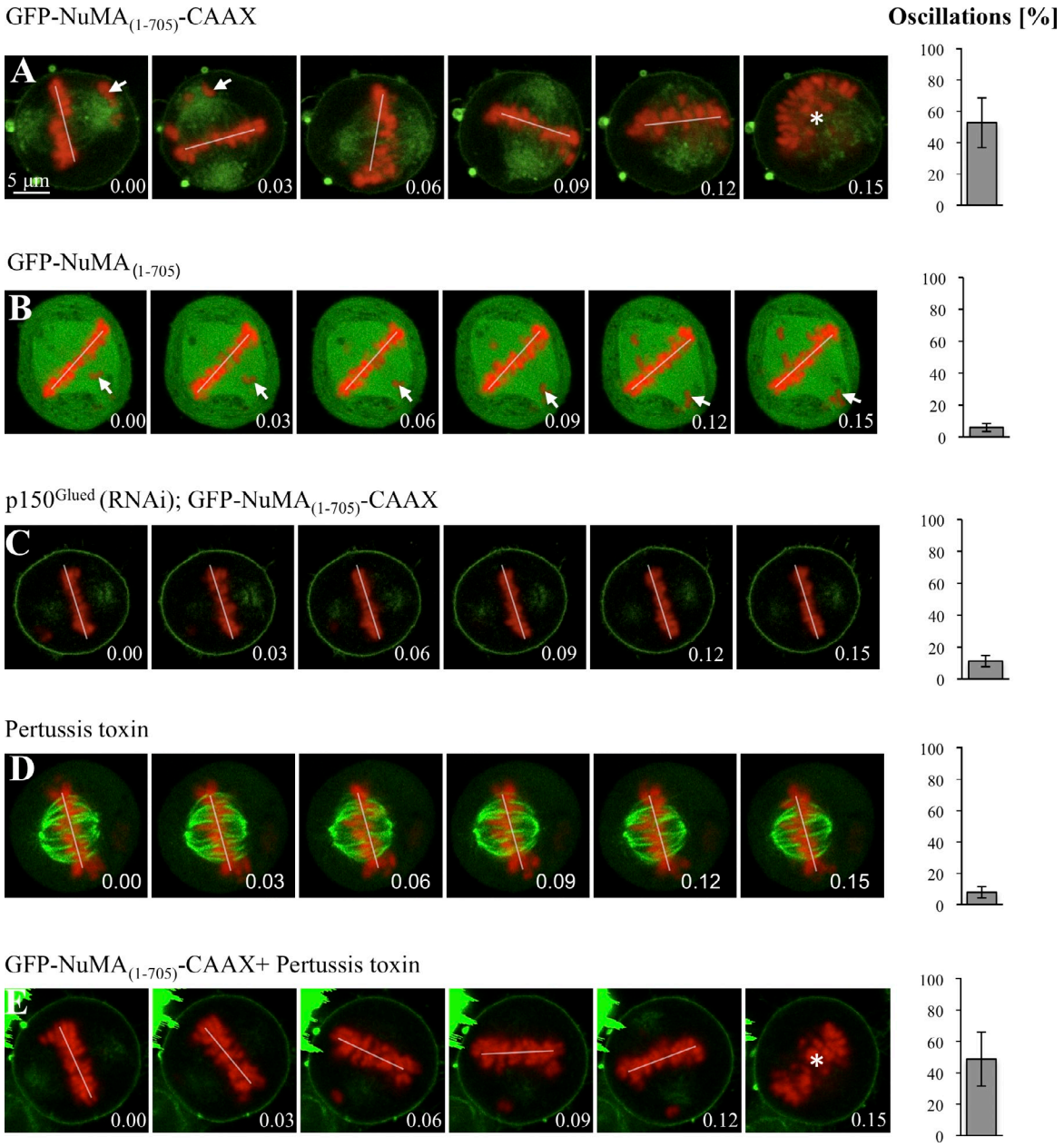

Figure 7. **Dynein anchored at the plasma membrane is sufficient for directing spindle positioning in HeLa cells.** (A–E) Images from time-lapse microscopy of metaphase HeLa Kyoto cells stably expressing GFP–α-tubulin as well as mCherry-H2B, transfected with GFP-NuMA(1–705)-CAAX (A), GFP-NuMA(1–705) (B), or GFP-NuMA(1–705)-CAAX and p150^{Glued} siRNAs (C), treated with pertussis toxin (D), or transfected with GFP-NuMA(1–705)-CAAX and also treated with pertussis toxin (E; see also corresponding Videos 7 and 8). Arrows point to misaligned chromosomes. Spindle positioning is monitored as explained for Fig. 2, with time indicated in hours and minutes. Given that chromosome congression was impaired upon GFP-NuMA(1–705)-CAAX overexpression, we also analyzed spindle oscillations using the GFP–α-tubulin signal in this case, with an indistinguishable outcome (oscillations 52 ± 7% SEM). 10 cells were analyzed for each condition. The extent of spindle oscillations upon overexpression of GFP-NuMA(1–705)-CAAX does not differ statistically from that upon overexpression of GFP-NuMA(1–705)-CAAX plus pertussis toxin (A vs. E, two-tailed Student's *t* tests; P = 0.39). Similarly, the values in GFP-NuMA(1–705)-CAAX and p150^{Glued} siRNA (C), as well GFP-NuMA(1–705) (B), are not statistically different from those in the control condition (Fig. 2 A); P = 0.74 and P = 0.20, respectively. In contrast, the values in GFP-NuMA(1–705)-CAAX and p150^{Glued} siRNA (C) are statistically different from those of GFP-NuMA(1–705)-CAAX overexpression alone (A; P < 0.0005). The position of chromosomes is indicated by a white line when chromosomes are within the imaging plane and by an asterisk when the metaphase plate is no longer in the plane of view.

p50/dynamitin (Echeverri et al., 1996; Neumann et al., 2010). In addition to the recently developed dynein inhibitor ciliobrevin (Firestone et al., 2012), the region described here widens the experimental palette to modulate dynein activity, offering the unique advantage of spatial control to redirect the motor complex to distinct cellular locations at will.

The ternary complex serves to anchor dynein to the plasma membrane and thus directs spindle positioning

Although it was known before our work that ternary complex components and dynein are important for spindle positioning, the exact nature of their relationship was not clear. Conceivably,

ternary complex components themselves could have participated more directly in spindle positioning, especially because Gα proteins purified from bovine brain can modulate microtubule dynamics (reviewed by Willard et al., 2004). Similarly, because NuMA and related proteins can bind to microtubules (Haren and Merdes, 2002; Bowman et al., 2006), they could have impacted spindle positioning directly by influencing microtubule behavior. We demonstrated in this study that spindle oscillations, which likely reflect pulling forces acting on astral microtubules, occur when dynein is targeted to the plasma membrane, and this is irrespective of the ternary complex being functional. Although we cannot exclude the possibility that ternary complex components contribute to spindle positioning in a minor manner, these findings strongly suggest instead that they merely serve to deliver and anchor appropriate levels of the dynein complex to the plasma membrane.

What are the mechanisms that regulate the availability of ternary complex components and, as a result, of dynein at the plasma membrane? In HeLa cells, phosphatidylinositol(3,4,5)P_3 modulates the levels of dynein at the plasma membrane, as well as spindle positioning (Toyoshima et al., 2007). It will be interesting to determine whether phosphatidylinositol(3,4,5)P_3 alters the distribution of ternary complex components to influence plasma membrane dynein distribution in human cells. Intriguingly, in *C. elegans* embryos, the casein kinase CSNK-1 negatively regulates levels of phosphatidylinositol(4,5)P_2 and results in the presence of more GPR-1/2 and LIN-5 at the plasma membrane, as well as excess forces pulling on astral microtubules (Panbianco et al., 2008). In the nematode, other components that modulate the presence of ternary complex components, and thus presumably of dynein, at the plasma membrane include the negative regulators Gβγ and the DEP domain–containing protein LET-99, as well as positive regulators such as the Gα-interacting protein RIC-8 and the protein phosphatase PPH-6 (Tsou et al., 2003; Afshar et al., 2004, 2010; Thyagarajan et al., 2011). In addition to spatial regulation, the ternary complex contributes to temporal regulation, as exemplified in human cells by the fact that NuMA, being nuclear during interphase, cannot interact with dynein during the bulk of the cell cycle. Similarly, LGN expression varies across the cell cycle, being maximal during mitosis (Whitfield et al., 2002; Du and Macara, 2004). Additional temporal regulation may be provided by post-translational modifications of ternary complex components.

Dynein activity at the plasma membrane

How does dynein act at the plasma membrane to direct spindle positioning? In *C. elegans* one-cell stage embryos, both dynein and microtubule depolymerization are important for generating pulling forces (Nguyen-Ngoc et al., 2007). Recent findings in vitro indicate that purified dynein coated on the edges of microfabricated chambers can interact with the plus end of microtubules and trigger catastrophes (Laan et al., 2012). Furthermore, these in vitro experiments also demonstrate that the intrinsic properties of dynein–microtubule interactions are sufficient to position a microtubule aster in the center of a microfabricated chamber. Our in vivo work with human cells is compatible with these in vitro results because we found that dynein at the plasma membrane is sufficient to direct spindle positioning independently of the ternary complex. It will be interesting to analyze microtubule dynamics in mitotic cells expressing GFP-NuMA (1–705)-CAAX to monitor the influence of plasma membrane dynein on microtubules. These and related approaches should help further clarify the mechanisms by which the presence of dynein at the cell cortex dictates proper spindle positioning in metazoan organisms.

Materials and methods

Cell culture, cell synchronization, and transfection

HeLa cells expressing GFP-Centrin 1 (a gift from M. Bornens, Institut Curie, Paris, France; Piel et al., 2000), HeLa cells expressing multifunctional GFP-IC74 (a gift from M. Takashi, Juntendo University School of Medicine, Tokyo, Japan; Kobayashi and Murayama, 2009), HeLa Kyoto cells expressing EGFP–α-tubulin and mCherry-H2B (a gift from D. Gerlich, Institute of Molecular Biotechnology, Vienna, Austria; Schmitz et al., 2010), and RPE-1 cells were all cultured in high-glucose DME with GlutaMAX (Invitrogen) and DME-F12 (Invitrogen) media supplemented with 10% FCS in a humidified 5% CO_2 incubator at 37°C. For monitoring spindle positioning in fixed specimens, cells were grown on coverslips uniformly coated with fibronectin (354088; BD) and synchronized using a double thymidine block. In brief, cells were incubated with 2 mM thymidine for 17 h, released for 8 h, and again incubated with 2 mM thymidine for 17 h. Cells were then released and fixed after 10 h, when a maximum number of cells were in mitosis. For analyzing Golgi localization on L-shape micropatterns, cells were transferred to L-shape micropatterns (CYTOO SA) 36 h after transfection. For siRNA experiments, ∼100,000 cells were seeded either on fibronectin-coated coverslips or regular glass coverslips in 6-well plates. 6 µl of 20-µM siRNA in 100 µl OptiMEM medium (Invitrogen) and 4 µl Lipofectamine RNAiMAX (Invitrogen) in 100 µl OptiMEM were incubated in parallel for 5 min, mixed for 20 min, and then added to 2.5 ml medium per well. For plasmid transfections, cells were seeded at 80–90% confluency. 4 µg plasmid DNA in 100 µl OptiMEM and 4 µl Lipofectamine 2000 (Invitrogen) in 100 µl OptiMEM were incubated in parallel for 5 min, mixed for 20 min, and added to each well. 80–95% transfection efficiency was routinely achieved as monitored by GFP staining.

Plasmids and RNAi

All NuMA fragments were constructed using full-length NuMA (a gift from A. Merdes, Université de Toulouse, Toulouse, France) as a template with appropriate PCR primer pairs. The amplified products were subcloned into pcDNA3-GFP (Merdes et al., 2000). GFP-NuMA(1–705)-CAAX was created by adding the CAAX polybasic sequence from K-ras4B (KKKKKKSKTKCVIM) at the C terminus of NuMA(1–705) using appropriate primer pairs and again subcloning the resulting amplified product into pcDNA3-GFP. The mutant in human $Gαi_1$ lacking the consensus myristoylation and palmitoylation sites at the N terminus (GC) was generated using full-length $Gαi_1$ (a gift from Q. Du, Georgia Health Science University, Augusta, GA) as a template and subcloning the PCR product into the YFP-carrying vector pKVenus (Nagai et al., 2002).

Double-stranded siRNA oligonucleotides were synthesized with the sequences 5′-UAGGAAAUCAUGAUCAAGCAA-3′ (LGN siRNA; QIAGEN), 5′-AAGGGCGCAAACAGAGCACUA-3′ (NuMA siRNA; QIAGEN), and 5′-CAGGUGGGUGUACAUUACGAA-3′ (DYNC1H1 siRNA; QIAGEN). An additional siRNA was tested for LGN and DYNC1HI, with a similar impact on spindle positioning. Strong depletion of LGN by two independent siRNAs led to many mitotic cells adopting a flattened morphology; only round cells were scored for spindle positioning on uniform fibronectin, which may explain discrepancies on this point with a previous study (Matsumura et al., 2012). For NuMA depletion, cells were treated a second time with siRNAs 48 h after the initial transfection and analyzed 48 h thereafter. For GFP-NuMA(1–705)-CAAX overexpression upon NuMA depletion, cells were treated with NuMA siRNA as mentioned in the previous sentence for 60 h before transfection with GFP-NuMA(1–705)-CAAX; cells were analyzed 36 h thereafter. Depletion of Rae1 was performed using a double-stranded siRNA oligonucleotide with the sequence 5′-CUCAGCAGUAACCAAGCGAUACAGA-3′ (Rae1 siRNA; Stealth RNAi; Invitrogen). Cells were incubated with pertussis toxin (181214A1; List Biological Laboratories, Inc.) at 400 ng/ml for 4 h before analysis.

Spindle positioning assay

The angle of the metaphase spindle with respect to the fibronectin substratum was determined as previously described (Toyoshima and Nishida, 2007). In brief, cells were stained with γ-tubulin antibodies to mark spindle poles and counterstained with 1 µg/ml Hoechst 33342 (Sigma-Aldrich) to mark chromosomes. Stacks of confocal images 0.4 µm apart were acquired, and the distances between the two spindle poles in z and in xy were determined using Imaris (Bitplane, Inc.). The spindle angle to the substratum was then calculated using inverse trigonometry.

Indirect immunofluorescence and time-lapse imaging of HeLa cells

For immunofluorescence, cells were fixed in −20°C methanol for 7–10 min and washed in PBS–0.05% Triton X-100 (PBST). After blocking in 1% BSA in PBST for 1 h, cells were incubated with primary antibodies overnight at 4°C. After three washes in PBST for 5 min, cells were incubated with secondary antibodies for 1 h at room temperature, stained with 1 µg/ml Hoechst 33342, washed three times for 5 min in PBST, and mounted. Primary antibodies were 1:300 rabbit anti-LGN (HPA007327; Sigma-Aldrich), 1:300 mouse anti-p150^{Glued} (612709; Transduction Laboratories), 1:2,000 mouse anti–γ-tubulin (GTU88; Sigma-Aldrich), 1:500 mouse anti-58K (AB27043; Abcam), 1:100 mouse anti-DIC (D5167; Sigma-Aldrich), 1:300 rabbit anti–GOA-1 (Afshar et al., 2004), 1:100 rabbit anti–DHC-1 (Gönczy et al., 1999), 1:300 mouse anti–α-tubulin (DM1a; Sigma-Aldrich), 1:2,000 mouse anti–γ-tubulin (GTU88; Sigma-Aldrich), 1:300 mouse anti-GFP (MAB3580; EMD Millipore), and 1:200 rabbit anti-GFP (a gift from V. Simanis, Swiss Federal Institute of Technology Lausanne, Lausanne, Switzerland). Secondary antibodies were Alexa Fluor 488–coupled anti–mouse, 1:500 Alexa Fluor 488–coupled anti–rabbit, Alexa Fluor 568–coupled anti–mouse, and Alexa Fluor 568–coupled anti–rabbit, all used at 1:500. Confocal images were acquired on a confocal microscope (LSM 710; Carl Zeiss) equipped with charge-coupled device camera (black and white; AxioCam MRm; Carl Zeiss) with a 63×, NA 1.0 oil objective and processed in ImageJ (National Institutes of Health) and Photoshop (Adobe), maintaining relative image intensities.

Time-lapse microscopy was conducted on a confocal microscope (LSM 700) equipped with charge-coupled device camera (black and white AxioCam MRm) with a 40×, NA 1.3 oil objective, using a Hi-Q4 dish (Ibidi) at 5% CO_2, 37°C, and 90% humidity. Images were acquired every 3 min, capturing four to five sections (7 µm apart) at each time point. Time-lapse figures and videos were obtained using a single confocal section of the z stack.

Immunoprecipitation and immunoblotting

For coimmunoprecipitations, 3 mg cell lysate was incubated with 50 µl Ni–nitriloacetic acid beads (QIAGEN) or 30 µl GFP-Trap agarose beads (ChromoTek) in lysis buffer (10 mM Tris, pH 7.5, 150 mM NaCl, 0.5% NP-40, 0.5 mM EDTA, 10 mM β-glycerophosphate, 5 mM NaF, 0.1 mM ATP, and EDTA-free protease inhibitor tablet [Complete; Roche]) for 4 h at 4°C. After extensive washing in wash buffer (10 mM Tris, pH 7.5, 150 mM NaCl, 0.5 mM EDTA, 10 mM β-glycerophosphate, 5 mM NaF, 0.1 mM ATP, and Complete EDTA-free protease inhibitor tablet), the beads were denatured at 95°C in 2× SDS buffer and analyzed by SDS-PAGE and immunoblotting. For immunoblotting, 1:2,000 mouse anti-GFP (MAB3580), 1:1,000 rabbit anti-NuMA (Santa Cruz Biotechnology, Inc.), and 1:10,000 mouse antiactin (MAB8172; Abnova) were used.

Nematode strains, RNAi, and indirect immunofluorescence

Transgenic worms expressing YFP–GPR-1 (strain TH242; a gift from H. Bringmann, Max-Planck-Institut, Göttingen, Germany; Redemann et al., 2011) were maintained at 24°C. The *goa-1(n1134)* (Mendel et al., 1995) and *goa-1(sa734)* (Robatzek and Thomas, 2000) mutants were maintained at 16°C. The *gpa-16(RNAi)* and *dhc-1(RNAi)* feeding strains were obtained from the ORFeome RNAi library (a gift from M. Vidal, Dana Farber Cancer Institute, Boston, MA). *C. elegans* mutant strains were obtained from the *Caenorhabditis* Genetics Center, which is funded by the National Institutes of Health National Center for Research Resources. Mild *dhc-1(RNAi)* in YFP–GPR-1 was performed by feeding L4 animals at 20°C for 12–15 h. *gpa-16(RNAi)* in *goa-1(n1134)* or *goa-1(sa734)* were performed by feeding L3 animals at 20°C for 36 h. For indirect immunofluorescence, embryos were fixed in methanol at −20°C for 1 h followed by incubation with primary antibodies for 4 h at room temperature. Secondary antibodies were incubated for 1 h at room temperature, and slides were stained with 1 µg/µl Hoechst 33258 to visualize DNA.

Online supplemental material

Fig. S1 shows that knockdown of ternary complex (NuMA–LGN–Gαi) components by siRNAs or inactivation of Gαi by pertussis toxin results in spindle positioning defects on a uniform fibronectin substrate. Fig. S2 shows that dynein function is necessary for ternary complex–induced spindle oscillations in HeLa cells. Fig. S3 shows that NuMA can interact with dynein, as well as the localization of GFP-NuMA(1–705), GFP-NuMA(706–1410), or GFP-NuMA(1,411–2,115), in interphase and mitotic cells. Fig. S4 shows that depleting Rae1 by siRNAs does not prevent the inhibitory effect of GFP-NuMA(1–705) on dynein function. Fig. S5 shows that overexpression of GFP-NuMA(1–705)-CAAX results in an increased fraction of binucleate/multinucleate cells as well as to a dispersal of chromosomes, which is accompanied by loss of p150^{Glued} at kinetochores. Video 1 shows a HeLa Kyoto cell stably expressing GFP–α-tubulin as well as mCherry-H2B and transfected with YFP, Gαi$_1$-YFP, and YFP-LGN. Video 2 shows a HeLa Kyoto cell stably expressing GFP–α-tubulin as well as mCherry-H2B and transfected with YFP and YFP-LGN. Video 3 shows metaphase spindle movements in HeLa cells overexpressing Gαi$_1$-YFP or YFP-LGN and treated with p150^{Glued} siRNAs or DYNC1H1 siRNAs. Video 4 shows metaphase spindle movements in HeLa cells overexpressing Gαi$_1$-Δmyr-YFP. Video 5 shows spindle positioning in wild-type, YFP–GPR-1, and YFP–GPR-1 *dhc-1(RNAi)* one-cell stage *C. elegans* embryos. Video 6 shows spindle positioning in wild-type, *goa-1(n1134) gpa-16(RNAi)*, and *goa-1(sa734) gpa-16(RNAi)* one-cell stage *C. elegans* embryos. Video 7 shows metaphase spindle movements in HeLa cells overexpressing GFP-NuMA(1–705)-CAAX and GFP-NuMA(1–705) or a cell transfected with GFP-NuMA(1–705)-CAAX plus p150^{Glued} siRNAs. Video 8 shows metaphase spindle movements in HeLa cells treated with pertussis toxin or transfected with GFP-NuMA(1–705)-CAAX plus treated with pertussis toxin. Online supplemental material is available at http://www.jcb.org/cgi/content/full/jcb.201203166/DC1.

We thank Virginie Hachet, Fernando R. Balestra, Kalyani Thyagarajan, Katayoun Afshar, and Sveta Chakrabarti for useful comments on the manuscript. We also thank the Swiss Federal Institute of Technology School of Life Sciences microscopy core facility for advice in image acquisition and analysis.

S. Kotak held a postdoctoral fellowship from the European Molecular Biology Organization (ALTF-366-2009). This work was supported also by grants to P. Gönczy from the Swiss National Science Foundation (3100A0-102087 and 3100A0-122500/1).

Submitted: 30 March 2012
Accepted: 30 August 2012

References

Afshar, K., F.S. Willard, K. Colombo, C.A. Johnston, C.R. McCudden, D.P. Siderovski, and P. Gönczy. 2004. RIC-8 is required for GPR-1/2-dependent Galpha function during asymmetric division of *C. elegans* embryos. *Cell*. 119:219–230. http://dx.doi.org/10.1016/j.cell.2004.09.026

Afshar, K., M.E. Werner, Y.C. Tse, M. Glotzer, and P. Gönczy. 2010. Regulation of cortical contractility and spindle positioning by the protein phosphatase 6 PPH-6 in one-cell stage *C. elegans* embryos. *Development*. 137:237–247. http://dx.doi.org/10.1242/dev.042754

Bowman, S.K., R.A. Neumüller, M. Novatchkova, Q. Du, and J.A. Knoblich. 2006. The *Drosophila* NuMA Homolog Mud regulates spindle orientation in asymmetric cell division. *Dev. Cell*. 10:731–742. http://dx.doi.org/10.1016/j.devcel.2006.05.005

Burkhardt, J.K., C.J. Echeverri, T. Nilsson, and R.B. Vallee. 1997. Overexpression of the dynamitin (p50) subunit of the dynactin complex disrupts dynein-dependent maintenance of membrane organelle distribution. *J. Cell Biol.* 139:469–484. http://dx.doi.org/10.1083/jcb.139.2.469

Colombo, K., S.W. Grill, R.J. Kimple, F.S. Willard, D.P. Siderovski, and P. Gönczy. 2003. Translation of polarity cues into asymmetric spindle positioning in *Caenorhabditis elegans* embryos. *Science*. 300:1957–1961. http://dx.doi.org/10.1126/science.1084146

Couwenbergs, C., J.C. Labbé, M. Goulding, T. Marty, B. Bowerman, and M. Gotta. 2007. Heterotrimeric G protein signaling functions with dynein to promote spindle positioning in *C. elegans*. *J. Cell Biol.* 179:15–22. http://dx.doi.org/10.1083/jcb.200707085

Du, Q., and I.G. Macara. 2004. Mammalian Pins is a conformational switch that links NuMA to heterotrimeric G proteins. *Cell*. 119:503–516. http://dx.doi.org/10.1016/j.cell.2004.10.028

Echeverri, C.J., B.M. Paschal, K.T. Vaughan, and R.B. Vallee. 1996. Molecular characterization of the 50-kD subunit of dynactin reveals function for the complex in chromosome alignment and spindle organization during mitosis. *J. Cell Biol.* 132:617–633. http://dx.doi.org/10.1083/jcb.132.4.617

Firestone, A.J., J.S. Weinger, M. Maldonado, K. Barlan, L.D. Langston, M. O'Donnell, V.I. Gelfand, T.M. Kapoor, and J.K. Chen. 2012. Small-molecule inhibitors of the AAA+ ATPase motor cytoplasmic dynein. *Nature*. 484:125–129. http://dx.doi.org/10.1038/nature10936

Gönczy, P. 2008. Mechanisms of asymmetric cell division: flies and worms pave the way. *Nat. Rev. Mol. Cell Biol.* 9:355–366. http://dx.doi.org/10.1038/nrm2388

Gönczy, P., S. Pichler, M. Kirkham, and A.A. Hyman. 1999. Cytoplasmic dynein is required for distinct aspects of MTOC positioning, including centrosome separation, in the one cell stage *Caenorhabditis elegans* embryo. *J. Cell Biol.* 147:135–150. http://dx.doi.org/10.1083/jcb.147.1.135

Gotta, M., and J. Ahringer. 2001. Distinct roles for Galpha and Gbetagamma in regulating spindle position and orientation in *Caenorhabditis elegans* embryos. *Nat. Cell Biol.* 3:297–300. http://dx.doi.org/10.1038/35060092

Gotta, M., Y. Dong, Y.K. Peterson, S.M. Lanier, and J. Ahringer. 2003. Asymmetrically distributed *C. elegans* homologs of AGS3/PINS control spindle position in the early embryo. *Curr. Biol.* 13:1029–1037. http://dx.doi.org/10.1016/S0960-9822(03)00371-3

Gueth-Hallonet, C., K. Weber, and M. Osborn. 1996. NuMA: a bipartite nuclear location signal and other functional properties of the tail domain. *Exp. Cell Res.* 225:207–218. http://dx.doi.org/10.1006/excr.1996.0171

Harborth, J., K. Weber, and M. Osborn. 1995. Epitope mapping and direct visualization of the parallel, in-register arrangement of the double-stranded coiled-coil in the NuMA protein. *EMBO J.* 14:2447–2460.

Harborth, J., J. Wang, C. Gueth-Hallonet, K. Weber, and M. Osborn. 1999. Self assembly of NuMA: multiarm oligomers as structural units of a nuclear lattice. *EMBO J.* 18:1689–1700. http://dx.doi.org/10.1093/emboj/18.6.1689

Haren, L., and A. Merdes. 2002. Direct binding of NuMA to tubulin is mediated by a novel sequence motif in the tail domain that bundles and stabilizes microtubules. *J. Cell Sci.* 115:1815–1824.

Kardon, J.R., and R.D. Vale. 2009. Regulators of the cytoplasmic dynein motor. *Nat. Rev. Mol. Cell Biol.* 10:854–865. http://dx.doi.org/10.1038/nrm2804

Kimura, K., and A. Kimura. 2011. Intracellular organelles mediate cytoplasmic pulling force for centrosome centration in the *Caenorhabditis elegans* early embryo. *Proc. Natl. Acad. Sci. USA*. 108:137–142. http://dx.doi.org/10.1073/pnas.1013275108

Kiyomitsu, T., and I.M. Cheeseman. 2012. Chromosome- and spindle-pole-derived signals generate an intrinsic code for spindle position and orientation. *Nat. Cell Biol.* 14:311–317. http://dx.doi.org/10.1038/ncb2440

Knoblich, J.A. 2008. Mechanisms of asymmetric stem cell division. *Cell*. 132:583–597. http://dx.doi.org/10.1016/j.cell.2008.02.007

Kobayashi, T., and T. Murayama. 2009. Cell cycle-dependent microtubule-based dynamic transport of cytoplasmic dynein in mammalian cells. *PLoS ONE*. 4:e7827. http://dx.doi.org/10.1371/journal.pone.0007827

Laan, L., N. Pavin, J. Husson, G. Romet-Lemonne, M. van Duijn, M.P. López, R.D. Vale, F. Jülicher, S.L. Reck-Peterson, and M. Dogterom. 2012. Cortical dynein controls microtubule dynamics to generate pulling forces that position microtubule asters. *Cell*. 148:502–514. http://dx.doi.org/10.1016/j.cell.2012.01.007

Lechler, T., and E. Fuchs. 2005. Asymmetric cell divisions promote stratification and differentiation of mammalian skin. *Nature*. 437:275–280. http://dx.doi.org/10.1038/nature03922

Matsumura, S., M. Hamasaki, T. Yamamoto, M. Ebisuya, M. Sato, E. Nishida, and F. Toyoshima. 2012. ABL1 regulates spindle orientation in adherent cells and mammalian skin. *Nat Commun*. 3:626. http://dx.doi.org/10.1038/ncomms1634

Mendel, J.E., H.C. Korswagen, K.S. Liu, Y.M. Hajdu-Cronin, M.I. Simon, R.H. Plasterk, and P.W. Sternberg. 1995. Participation of the protein Go in multiple aspects of behavior in *C. elegans*. *Science*. 267:1652–1655. http://dx.doi.org/10.1126/science.7886455

Merdes, A., K. Ramyar, J.D. Vechio, and D.W. Cleveland. 1996. A complex of NuMA and cytoplasmic dynein is essential for mitotic spindle assembly. *Cell*. 87:447–458. http://dx.doi.org/10.1016/S0092-8674(00)81365-3

Merdes, A., R. Heald, K. Samejima, W.C. Earnshaw, and D.W. Cleveland. 2000. Formation of spindle poles by dynein/dynactin-dependent transport of NuMA. *J. Cell Biol.* 149:851–862. http://dx.doi.org/10.1083/jcb.149.4.851

Nagai, T., K. Ibata, E.S. Park, M. Kubota, K. Mikoshiba, and A. Miyawaki. 2002. A variant of yellow fluorescent protein with fast and efficient maturation for cell-biological applications. *Nat. Biotechnol.* 20:87–90. http://dx.doi.org/10.1038/nbt0102-87

Neumann, B., T. Walter, J.K. Hériché, J. Bulkescher, H. Erfle, C. Conrad, P. Rogers, I. Poser, M. Held, U. Liebel, et al. 2010. Phenotypic profiling of the human genome by time-lapse microscopy reveals cell division genes. *Nature*. 464:721–727. http://dx.doi.org/10.1038/nature08869

Nguyen-Ngoc, T., K. Afshar, and P. Gönczy. 2007. Coupling of cortical dynein and G alpha proteins mediates spindle positioning in *Caenorhabditis elegans*. *Nat. Cell Biol.* 9:1294–1302. http://dx.doi.org/10.1038/ncb1649

Panbianco, C., D. Weinkove, E. Zanin, D. Jones, N. Divecha, M. Gotta, and J. Ahringer. 2008. A casein kinase 1 and PAR proteins regulate asymmetry of a PIP(2) synthesis enzyme for asymmetric spindle positioning. *Dev. Cell*. 15:198–208. http://dx.doi.org/10.1016/j.devcel.2008.06.002

Park, D.H., and L.S. Rose. 2008. Dynamic localization of LIN-5 and GPR-1/2 to cortical force generation domains during spindle positioning. *Dev. Biol.* 315:42–54. http://dx.doi.org/10.1016/j.ydbio.2007.11.037

Peyre, E., F. Jaouen, M. Saadaoui, L. Haren, A. Merdes, P. Durbec, and X. Morin. 2011. A lateral belt of cortical LGN and NuMA guides mitotic spindle movements and planar division in neuroepithelial cells. *J. Cell Biol.* 193:141–154. http://dx.doi.org/10.1083/jcb.201101039

Piel, M., P. Meyer, A. Khodjakov, C.L. Rieder, and M. Bornens. 2000. The respective contributions of the mother and daughter centrioles to centrosome activity and behavior in vertebrate cells. *J. Cell Biol.* 149:317–330. http://dx.doi.org/10.1083/jcb.149.2.317

Radulescu, A.E., and D.W. Cleveland. 2010. NuMA after 30 years: the matrix revisited. *Trends Cell Biol.* 20:214–222. http://dx.doi.org/10.1016/j.tcb.2010.01.003

Rapali, P., L. Radnai, D. Süveges, V. Harmat, F. Tölgyesi, W.Y. Wahlgren, G. Katona, L. Nyitray, and G. Pál. 2011. Directed evolution reveals the binding motif preference of the LC8/DYNLL hub protein and predicts large numbers of novel binders in the human proteome. *PLoS ONE*. 6:e18818. http://dx.doi.org/10.1371/journal.pone.0018818

Redemann, S., S. Schloissnig, S. Ernst, A. Pozniakowsky, S. Ayloo, A.A. Hyman, and H. Bringmann. 2011. Codon adaptation-based control of protein expression in *C. elegans*. *Nat. Methods*. 8:250–252. http://dx.doi.org/10.1038/nmeth.1565

Robatzek, M., and J.H. Thomas. 2000. Calcium/calmodulin-dependent protein kinase II regulates *Caenorhabditis elegans* locomotion in concert with a G(o)/G(q) signaling network. *Genetics*. 156:1069–1082.

Schmitz, M.H., M. Held, V. Janssens, J.R. Hutchins, O. Hudecz, E. Ivanova, J. Goris, L. Trinkle-Mulcahy, A.I. Lamond, I. Poser, et al. 2010. Live-cell imaging RNAi screen identifies PP2A-B55alpha and importin-beta1 as key mitotic exit regulators in human cells. *Nat. Cell Biol.* 12:886–893. http://dx.doi.org/10.1038/ncb2092

Siller, K.H., and C.Q. Doe. 2009. Spindle orientation during asymmetric cell division. *Nat. Cell Biol.* 11:365–374. http://dx.doi.org/10.1038/ncb0409-365

Srinivasan, D.G., R.M. Fisk, H. Xu, and S. van den Heuvel. 2003. A complex of LIN-5 and GPR proteins regulates G protein signaling and spindle function in *C. elegans*. *Genes Dev.* 17:1225–1239. http://dx.doi.org/10.1101/gad.1081203

Théry, M., V. Racine, A. Pépin, M. Piel, Y. Chen, J.B. Sibarita, and M. Bornens. 2005. The extracellular matrix guides the orientation of the cell division axis. *Nat. Cell Biol.* 7:947–953. http://dx.doi.org/10.1038/ncb1307

Thyagarajan, K., K. Afshar, and P. Gönczy. 2011. Polarity mediates asymmetric trafficking of the Gbeta heterotrimeric G-protein subunit GPB-1 in *C. elegans* embryos. *Development*. 138:2773–2782. http://dx.doi.org/10.1242/dev.063354

Toyoshima, F., and E. Nishida. 2007. Integrin-mediated adhesion orients the spindle parallel to the substratum in an EB1- and myosin X-dependent manner. *EMBO J.* 26:1487–1498. http://dx.doi.org/10.1038/sj.emboj.7601599

Toyoshima, F., S. Matsumura, H. Morimoto, M. Mitsushima, and E. Nishida. 2007. PtdIns(3,4,5)P3 regulates spindle orientation in adherent cells. *Dev. Cell*. 13:796–811. http://dx.doi.org/10.1016/j.devcel.2007.10.014

Tsou, M.F., A. Hayashi, and L.S. Rose. 2003. LET-99 opposes Galpha/GPR signaling to generate asymmetry for spindle positioning in response to PAR and MES-1/SRC-1 signaling. *Development*. 130:5717–5730. http://dx.doi.org/10.1242/dev.00790

Whitfield, M.L., G. Sherlock, A.J. Saldanha, J.I. Murray, C.A. Ball, K.E. Alexander, J.C. Matese, C.M. Perou, M.M. Hurt, P.O. Brown, and D. Botstein. 2002. Identification of genes periodically expressed in the human cell cycle and their expression in tumors. *Mol. Biol. Cell*. 13:1977–2000. http://dx.doi.org/10.1091/mbc.02-02-0030.

Willard, F.S., R.J. Kimple, and D.P. Siderovski. 2004. Return of the GDI: the GoLoco motif in cell division. *Annu. Rev. Biochem.* 73:925–951. http://dx.doi.org/10.1146/annurev.biochem.73.011303.073756

Williams, S.E., S. Beronja, H.A. Pasolli, and E. Fuchs. 2011. Asymmetric cell divisions promote Notch-dependent epidermal differentiation. *Nature*. 470:353–358. http://dx.doi.org/10.1038/nature09793

Wong, R.W., G. Blobel, and E. Coutavas. 2006. Rae1 interaction with NuMA is required for bipolar spindle formation. *Proc. Natl. Acad. Sci. USA*. 103:19783–19787. http://dx.doi.org/10.1073/pnas.0609582104

Woodard, G.E., N.N. Huang, H. Cho, T. Miki, G.G. Tall, and J.H. Kehrl. 2010. Ric-8A and Gi alpha recruit LGN, NuMA, and dynein to the cell cortex to help orient the mitotic spindle. *Mol. Cell. Biol.* 30:3519–3530. http://dx.doi.org/10.1128/MCB.00394-10

Wühr, M., S. Dumont, A.C. Groen, D.J. Needleman, and T.J. Mitchison. 2009. How does a millimeter-sized cell find its center? *Cell Cycle*. 8:1115–1121. http://dx.doi.org/10.4161/cc.8.8.8150

Zheng, Z., H. Zhu, Q. Wan, J. Liu, Z. Xiao, D.P. Siderovski, and Q. Du. 2010. LGN regulates mitotic spindle orientation during epithelial morphogenesis. *J. Cell Biol.* 189:275–288. http://dx.doi.org/10.1083/jcb.200910021